Elasto/Visco-Plastic Deformation of Multi-Layered Moderately Thick Shells of Revolution *

Shigeo TAKEZONO **, Katsumi TAO **
and Kiyoyuki TANI ***

This paper is concerned with an analytical formulation and a numerical solution of the elasto/visco-plastic problems of multi-layered moderately thick shells of revolution under asymmetrical loads with application to a cylindrical shell. The analytical formulation is developed by extending the Reissner-Naghdi theory on elastic shells. It is assumed that the total strain rates are composed of an elastic part and a part due to visco-plasticity. The elastic strains are proportional to the stresses by Hooke's law. The visco-plastic strain rates are related to the stresses according to Perzyna's equation. As a numerical example, the elasto/visco-plastic deformation of a two-layered cylindrical shell composed of a titanium and a mild steel layer subjected to locally distributed loads is analyzed. Numerical computations are carried out for three cases of the ratio of the thickness of the titanium layer to the shell thickness. It is found from the computations that the stress distributions and the deformation vary significantly depending on the thickness ratio.

Key Words: Structural Analysis, Computational Mechanics, Laminated Construction, FDM, Elasto/Visco-Plasticity, Thick Shells

1. Introduction

Many investigations[1]~[11] of the elasto/visco-plastic deformation of shells of revolution have been conducted. These investigations, however, have been mostly concerned with the case of single-layered shells, and few studies on multi-layered shells composed of different materials have been reported in spite of their importance in engineering, with the exception of the study which the authors performed on thin shells[12].

In this paper, the authors study the elasto/visco-plastic deformation of multi-layered moderately thick shells of revolution under general asymmetrical loads. The equations of equilibrium and the relationships between strain and displacement are derived from the Reissner-Naghdi theory[13],[14] for elastic shells where a consideration on the effect of shear deformation is given. As the constitutive relation, Hooke's law is used in the linear elastic range, and the elasto/visco-plastic equations by Perzyna [15] are employed in the plastic range.

In the case of multi-layered shells, the relationships between the generalized stresses and strains are different from those of single-layered shells, and therefore the derived basic differential equations are also different.

The basic differential equations for incremental values are numerically solved by a finite difference method, and the solutions are obtained by a summation of the incremental values.

As a numerical example, the elasto/visco-plastic deformation of a simply supported two-layered cylindrical shell composed of a titanium and a mild steel layer subjected to locally distributed loads is analyzed. Numerical computations are carried out for three cases of the ratio of the thickness of the titanium layer to the shell thickness.

2. Analytical Formulations

2.1 Fundamental equations

If the middle surface of the shells of revolution is

* Received 21st May, 1990. Paper No.89-0476A
** Department of Energy Engineering, Toyohashi University of Technology, Tempaku-cho, Toyohashi 441, Japan
*** Nikko System Center Co.Ltd., Shinagawa-ku, Tokyo 141, Japan

given by $r=r(s)$, where r is the distance from the axis and s is the meridional distance measured from a boundary along the middle surface as shown in Fig.1, the relations among the nondimensional curvatures $\omega_\xi(=a/R_s)$, $\omega_\theta(=a/R_\theta)$ and the nondimensional radius $\rho(=r/a)$ become

$$\left.\begin{aligned}&\omega_\xi=-(\gamma'+\gamma^2)/\omega_\theta,\ \omega_\theta=\sqrt{1-(\rho')^2}/\rho\\&\omega_\theta'=\gamma(\omega_\xi-\omega_\theta),\ \rho''/\rho=-\omega_\xi\omega_\theta\\&\gamma=\rho'/\rho,\ \xi=s/a,\ (\ )'=d(\ )/d\xi\end{aligned}\right\}\quad(1)$$

where a is the reference length. An arbitrary point of the shell can be expressed in the orthogonal coordinate system (ξ, θ, ζ).

An application of the Reissner shell theory[13] to the shells of revolution and a differentiation of the equilibrium equation with time or load yield

$$\left.\begin{aligned}&\frac{\partial\dot N_\xi}{\partial\xi}+\gamma(\dot N_\xi-\dot N_\theta)+\frac{1}{\rho}\frac{\partial\dot N_{\theta\xi}}{\partial\theta}+\omega_\xi\dot Q_\xi+a\dot P_\xi=0\\&\frac{\partial\dot N_{\xi\theta}}{\partial\xi}+\gamma(\dot N_{\xi\theta}+\dot N_{\theta\xi})+\frac{1}{\rho}\frac{\partial\dot N_\theta}{\partial\theta}+\omega_\theta\dot Q_\theta+a\dot P_\theta=0\\&\frac{\partial\dot Q_\xi}{\partial\xi}+\gamma\dot Q_\xi+\frac{1}{\rho}\frac{\partial\dot Q_\theta}{\partial\theta}-(\omega_\xi\dot N_\xi+\omega_\theta\dot N_\theta)+a\dot P_\zeta=0\\&\dot Q_\xi-\frac{1}{a}\left[\frac{\partial\dot M_\xi}{\partial\xi}+\gamma(\dot M_\xi-\dot M_\theta)+\frac{1}{\rho}\frac{\partial\dot M_{\theta\xi}}{\partial\theta}\right]=0\\&\dot Q_\theta-\frac{1}{a}\left[\frac{\partial\dot M_{\xi\theta}}{\partial\xi}+\gamma(\dot M_{\xi\theta}+\dot M_{\theta\xi})+\frac{1}{\rho}\frac{\partial\dot M_\theta}{\partial\theta}\right]=0\end{aligned}\right\}\quad(2)$$

where the notations are shown in Fig. 1. P_ξ, P_θ and P_ζ are components of distributed loads per unit area of the middle surface, and these are connected with internal pressures $\{P_\xi^-, P_\theta^-, P_\zeta^-\}$ and external pressures $\{P_\xi^+, P_\theta^+, P_\zeta^+\}$ by the following relation :

$$\{P_\xi, P_\theta, P_\zeta\}=\{P_\xi^-, P_\theta^-, P_\zeta^-\}h^- -\{P_\xi^+, P_\theta^+, P_\zeta^+\}h^+\quad(3)$$

where

$$h^\pm=1\pm\frac{h}{2}\left(\frac{1}{R_s}+\frac{1}{R_\theta}\right)+\frac{h^2}{4}\frac{1}{R_sR_\theta}\quad(4)$$

The strain rates of the middle surface, $\dot\varepsilon_{\xi m}$, $\dot\varepsilon_{\theta m}$, $\dot\varepsilon_{\xi\theta m}$, are given by the displacements U_ξ, U_θ, U_ζ in the next equations[14]:

$$\left.\begin{aligned}&\dot\varepsilon_{\xi m}=\frac{1}{a}\left[\frac{\partial\dot U_\xi}{\partial\xi}+\omega_\xi\dot U_\zeta\right]\\&\dot\varepsilon_{\theta m}=\frac{1}{a}\left[\frac{1}{\rho}\frac{\partial\dot U_\theta}{\partial\theta}+\gamma\dot U_\xi+\omega_\theta\dot U_\zeta\right]\\&\dot\varepsilon_{\xi\theta m}=\frac{1}{2a}\left[\frac{1}{\rho}\frac{\partial\dot U_\xi}{\partial\theta}+\frac{\partial\dot U_\theta}{\partial\xi}-\gamma\dot U_\theta\right]\end{aligned}\right\}\quad(5)$$

where $\dot\varepsilon_{\xi\theta m}$ is half the usual engineering shear strain rate.

The relations between the bending distortions χ_ξ, χ_θ, $\chi_{\xi\theta}$, $\chi_{\theta\xi}$ and the displacements are[14]

$$\left.\begin{aligned}&\dot\chi_\xi=\frac{1}{a}\frac{\partial\dot\Phi_\xi}{\partial\xi},\ \dot\chi_\theta=\frac{1}{a}\left(\frac{1}{\rho}\frac{\partial\dot\Phi_\theta}{\partial\theta}+\gamma\dot\Phi_\xi\right)\\&\dot\chi_{\xi\theta}=\frac{1}{2a}\left(\frac{\partial\dot\Phi_\theta}{\partial\xi}-2\omega_\xi\dot\Phi_n\right)\\&\dot\chi_{\theta\xi}=\frac{1}{2a}\left(\frac{1}{\rho}\frac{\partial\dot\Phi_\xi}{\partial\theta}-\gamma\dot\Phi_\theta+2\omega_\theta\dot\Phi_n\right)\end{aligned}\right\}\quad(6)$$

where rotation rates $\dot\Phi_\xi$, $\dot\Phi_\theta$ and $\dot\Phi_n$ are

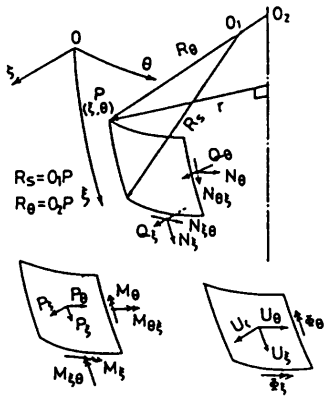

Fig. 1 Coordinates and notations

$$\left.\begin{aligned}&\dot\Phi_\xi=\frac{1}{a}\left(-\frac{\partial\dot U_\zeta}{\partial\xi}+\omega_\xi\dot U_\xi\right)+2\dot\varepsilon_{\xi\zeta m}\\&\dot\Phi_\theta=\frac{1}{a}\left(-\frac{1}{\rho}\frac{\partial\dot U_\zeta}{\partial\theta}+\omega_\theta\dot U_\theta\right)+2\dot\varepsilon_{\theta\zeta m}\\&\dot\Phi_n=\frac{1}{2a}\left(-\frac{1}{\rho}\frac{\partial\dot U_\xi}{\partial\theta}+\frac{\partial\dot U_\theta}{\partial\xi}+\gamma\dot U_\theta\right)\end{aligned}\right\}\quad(7)$$

The strain rates at the distance ζ from the middle surface are given as

$$\left.\begin{aligned}&\dot\varepsilon_\xi=(\dot\varepsilon_{\xi m}+\zeta\dot\chi_\xi)/L_\xi,\ \dot\varepsilon_\theta=(\dot\varepsilon_{\theta m}+\zeta\chi_\theta)/L_\theta\\&\dot\varepsilon_{\xi\theta}=\left\{\frac{1}{2}(\dot\varepsilon_{\xi\theta m}+\dot\Phi_n)+\zeta(\dot\chi_{\xi\theta}+\dot\Phi_n/R_s)\right\}\Big/L_\xi\\&\qquad+\frac{1}{2}(\dot\varepsilon_{\xi\theta m}-\dot\Phi_n)+\zeta(\dot\chi_{\theta\xi}-\dot\Phi_n/R_\theta)\Big\}\Big/L_\theta\\&\dot\varepsilon_{\xi\zeta}=\varepsilon_{\xi\zeta m}/L_\xi,\ \dot\varepsilon_{\theta\zeta}=\dot\varepsilon_{\theta\zeta m}/L_\theta\end{aligned}\right\}\quad(8)$$

where

$L_\xi=1+\zeta/R_s$, $L_\theta=1+\zeta/R_\theta$.

Now, we shall use the elasto/visco-plastic equations by Perzyna[15] for the constitutive relation

$$\dot\varepsilon_{ij}=\frac{1+\nu}{E}\dot S_{ij}+\frac{1-2\nu}{E}\dot S\delta_{ij}+\gamma_0<\Phi(F)>S_{ij}J_2^{-1/2}\quad(9)$$

where the dot denotes partial differentiation with respect to time ; ε_{ij}, S, S_{ij} and J_2 are strain, mean stress, deviatoric stress and the second invariant of the deviatoric stress, respectively ; and E, ν and γ_0 are Young's modulus, Poisson's ratio and the viscosity constant of the material. The symbol $\langle\Phi(F)\rangle$ is defined as follows :

$$<\Phi(F)>=0 : F\leqq 0,\ <\Phi(F)>=\Phi(F) : F>0\quad(10)$$

where function F is

$$F=(\bar\sigma-\sigma^*)/\sigma^*,\quad(11)$$

and $F=0$ denotes the von Mises yield surface, $\bar\sigma$ is the equivalent stress $(=\sqrt{3J_2})$ and σ^* is the statical stress determined from the elasto-plastic stress-strain relation in a usual tension test, and becomes the function of the equivalent plastic strain $\bar\varepsilon^{vp}$ in general.

In the present theory where the stress component σ_ζ normal to the middle surface can be assumed to be

neglected, the constitutive equations are written as follows :

$$\{\dot{\varepsilon}\}=[D]^{-1}\{\dot{\sigma}\}+\{\dot{\varepsilon}^{vp}\} \tag{12}$$

where

$$\{\dot{\varepsilon}\}=\{\dot{\varepsilon}_\ell,\ \dot{\varepsilon}_\theta,\ \dot{\varepsilon}_{\ell\theta},\ \dot{\varepsilon}_{\ell\zeta},\ \dot{\varepsilon}_{\theta\zeta}\}^T,\ \{\dot{\sigma}\}=\{\dot{\sigma}_\ell,\ \dot{\sigma}_\theta,\ \dot{\sigma}_{\ell\theta},\ \dot{\sigma}_{\ell\zeta},\ \dot{\sigma}_{\theta\zeta}\}^T$$

$$\left.\begin{aligned}\{\dot{\varepsilon}^{vp}\}&=\{\dot{\varepsilon}_\ell^{vp},\ \dot{\varepsilon}_\theta^{vp},\ \dot{\varepsilon}_{\ell\theta}^{vp},\ \dot{\varepsilon}_{\ell\zeta}^{vp},\ \dot{\varepsilon}_{\theta\zeta}^{vp}\}^T=\gamma_1<\Phi\left(\frac{\bar{\sigma}-\sigma^*}{\sigma^*}\right)>\frac{1}{\bar{\sigma}}\begin{bmatrix}1&-1/2&0&0&0\\-1/2&1&0&0&0\\0&0&3/2&0&0\\0&0&0&3/2&0\\0&0&0&0&3/2\end{bmatrix}\{\sigma\}\\ \gamma_1&=\frac{2}{\sqrt{3}}\gamma_0,\ [D]=\frac{E}{1-\nu^2}\begin{bmatrix}1&\nu&0&0&0\\\nu&1&0&0&0\\0&0&1-\nu&0&0\\0&0&0&1-\nu&0\\0&0&0&0&1-\nu\end{bmatrix}\end{aligned}\right\} \tag{13}$$

Substituting Eqs.(8) into Eqs.(12) and solving them for stress rates, the stress rates are given :

$$\left.\begin{aligned}\dot{\sigma}_\ell&=\frac{E}{1-\nu^2}\{(\dot{\varepsilon}_{\ell m}+\zeta\dot{\varkappa}_\ell)/L_\ell+\nu(\dot{\varepsilon}_{\theta m}+\zeta\dot{\varkappa}_\theta)/L_\theta\}-\dot{\sigma}_\ell^{vp}\\ \dot{\sigma}_\theta&=\frac{E}{1-\nu^2}\{(\dot{\varepsilon}_{\theta m}+\zeta\dot{\varkappa}_\theta)/L_\theta+\nu(\dot{\varepsilon}_{\ell m}+\zeta\dot{\varkappa}_\ell)/L_\ell\}-\dot{\sigma}_\theta^{vp}\\ \dot{\sigma}_{\ell\theta}&=\frac{E}{1+\nu}\left[\left\{\frac{1}{2}(\dot{\varepsilon}_{\ell\theta m}+\dot{\Phi}_n)+\zeta\left(\dot{\varkappa}_{\ell\theta}+\frac{\dot{\Phi}_n}{R_s}\right)\right\}/L_\ell+\left\{\frac{1}{2}(\dot{\varepsilon}_{\ell\theta m}-\dot{\Phi}_n)+\zeta\left(\dot{\varkappa}_{\theta\ell}-\frac{\dot{\Phi}_n}{R_\theta}\right)\right\}\Big/L_\theta\right]-\dot{\sigma}_{\ell\theta}^{vp}\\ \dot{\sigma}_{\ell\zeta}&=\frac{E}{1+\nu}\dot{\varepsilon}_{\ell\zeta m}/L_\ell-\dot{\sigma}_{\ell\zeta}^{vp},\ \dot{\sigma}_{\theta\zeta}=\frac{E}{1+\nu}\dot{\varepsilon}_{\theta\zeta m}/L_\theta-\dot{\sigma}_{\theta\zeta}^{vp}\end{aligned}\right\} \tag{14}$$

where

$$\{\dot{\sigma}^{vp}\}=\{\dot{\sigma}_\ell^{vp},\ \dot{\sigma}_\theta^{vp},\ \dot{\sigma}_{\ell\theta}^{vp},\ \dot{\sigma}_{\ell\zeta}^{vp},\ \dot{\sigma}_{\theta\zeta}^{vp}\}^T=[D]\{\dot{\varepsilon}^{vp}\} \tag{15}$$

By the use of Eqs.(14) with the approximation,

$$\frac{L_\theta}{L_\ell}\simeq 1-\left(\frac{1}{R_s}-\frac{1}{R_\theta}\right)\zeta+\frac{1}{R_s}\left(\frac{1}{R_s}-\frac{1}{R_\theta}\right)\zeta^2 \tag{16}$$

the rates of change of the resultant stresses and the resultant moments per unit length for the multi-layered shell (Fig. 2) may be expressed by the following :

$$\begin{Bmatrix}\dot{N}\\ \dot{M}\end{Bmatrix}=\int_{-h/2}^{h/2}[L]\begin{Bmatrix}\dot{\sigma}\\ \dot{\sigma}^*\zeta\end{Bmatrix}d\zeta=[A]\begin{Bmatrix}\dot{\varepsilon}_m\\ \dot{\varkappa}\\ \dot{\Phi}_n\end{Bmatrix}-\begin{Bmatrix}\dot{N}^{vp}\\ \dot{M}^{vp}\end{Bmatrix} \tag{17}$$

where

$$\{\dot{N}\}=\{\dot{N}_\ell,\ \dot{N}_\theta,\ \dot{N}_{\ell\theta},\ \dot{N}_{\theta\ell},\ \dot{Q}_\ell,\ \dot{Q}_\theta\}^T,\ \{\dot{M}\}=\{\dot{M}_\ell,\ \dot{M}_\theta,\ \dot{M}_{\ell\theta},\ \dot{M}_{\theta\ell}\}^T$$

$$\left.\begin{aligned}[L]&=\begin{bmatrix}L_1&0\\0&L_2\end{bmatrix},\ [L_1]=\begin{bmatrix}L_\theta&&&&\\&L_\ell&&0&\\&&L_\theta&&\\&&L_\ell&&\\&0&&L_\theta&\\&&&&L_\ell\end{bmatrix},\ [L_2]=\begin{bmatrix}L_\theta&&0\\&L_\ell&\\&&L_\theta\\0&&L_\ell\end{bmatrix}\end{aligned}\right\}$$

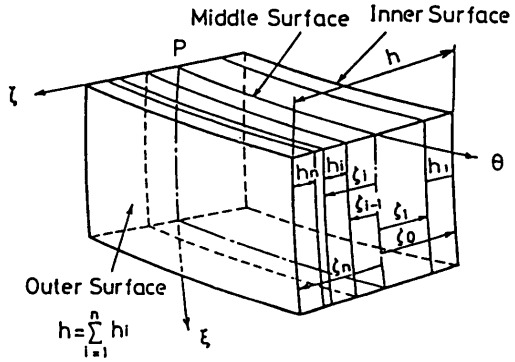

Fig. 2 Multi-layered shell element

$$(\{a_1, a_2, a_3, a_4, a_5\}^T)^*=\{a_1, a_2, a_3\}^T, \{\dot{\varepsilon}_m\}=\{\dot{\varepsilon}_{\xi m}, \dot{\varepsilon}_{\theta m}, \dot{\varepsilon}_{\xi\theta m}, \dot{\varepsilon}_{\xi\zeta m}, \dot{\varepsilon}_{\theta\zeta m}\}^T, \{\dot{x}\}=\{\dot{x}_\xi, \dot{x}_\theta, \dot{x}_{\xi\theta}, \dot{x}_{\theta\xi}\}^T \tag{18}$$

$$[A]=\sum_{i=1}^{n}[E_i][A_i] \tag{19}$$

$$[E_i]=\frac{E_i}{1-\nu_i^2}[1, 1, 1-\nu_i, 1-\nu_i, 1-\nu_i, 1-\nu_i, 1, 1, 1-\nu_i, 1-\nu_i] : \text{(diagonal matrix)} \tag{20}$$

$$[A_i]=\left[\begin{array}{ccccccccccc}
\zeta_{1,i}^*, & \nu_i\zeta_{1,i}, & 0, & 0, & 0, & \zeta_{2,i}^*, & \nu_i\zeta_{2,i}, & 0, & 0, & 0 & \\
\nu_i\zeta_{1,i}, & \zeta_{1,i}^{**}, & 0, & 0, & 0, & \nu_i\zeta_{2,i}, & \zeta_{2,i}^{**}, & 0, & 0, & 0 & \\
0, & 0, & \frac{1}{2}(\zeta_{1,i}^*+\zeta_{1,i}), & 0, & 0, & 0, & 0, & \zeta_{2,i}^*, & \zeta_{2,i}, & & (a)\\
0, & 0, & \frac{1}{2}(\zeta_{1,i}^{**}+\zeta_{1,i}), & 0, & 0, & 0, & 0, & \zeta_{2,i}, & \zeta_{2,i}^{**}, & & (b)\\
0, & 0, & 0, & 5/6\zeta_{1,i}^*, & 0, & 0, & 0, & 0, & 0, & 0 & \\
0, & 0, & 0, & 0, & 5/6\zeta_{1,i}^{**}, & 0, & 0, & 0, & 0, & 0 & \\
\zeta_{2,i}^*, & \nu_i\zeta_{2,i}, & 0, & 0, & 0, & \zeta_{3,i}^*, & \nu_i\zeta_{3,i}, & 0, & 0, & 0 & \\
\nu_i\zeta_{2,i}, & \zeta_{2,i}^{**}, & 0, & 0, & 0, & \nu_i\zeta_{3,i}, & \zeta_{3,i}^{**}, & 0, & 0, & 0 & \\
0, & 0, & \frac{1}{2}(\zeta_{2,i}^*+\zeta_{2,i}), & 0, & 0, & 0, & 0, & \zeta_{3,i}^*, & \zeta_{3,i}, & & (c)\\
0, & 0, & \frac{1}{2}(\zeta_{2,i}^{**}+\zeta_{2,i}), & 0, & 0, & 0, & 0, & \zeta_{3,i}, & \zeta_{3,i}^{**}, & & (d)
\end{array}\right]$$

$$(a)=\frac{1}{2}(\zeta_{1,i}^*-\zeta_{1,i})+\frac{\omega_\xi}{a}\zeta_{2,i}^*-\frac{\omega_\theta}{a}\zeta_{2,i}, \quad (b)=\frac{1}{2}(\zeta_{1,i}-\zeta_{1,i}^{**})+\frac{\omega_\xi}{a}\zeta_{2,i}-\frac{\omega_\theta}{a}\zeta_{2,i}^{**}$$

$$(c)=\frac{1}{2}(\zeta_{2,i}^*-\zeta_{2,i})+\frac{\omega_\xi}{a}\zeta_{3,i}^*-\frac{\omega_\theta}{a}\zeta_{3,i}, \quad (d)=\frac{1}{2}(\zeta_{2,i}-\zeta_{2,i}^{**})+\frac{\omega_\xi}{a}\zeta_{3,i}-\frac{\omega_\theta}{a}\zeta_{3,i}^{**} \tag{21}$$

$$\zeta_{n,i}=\frac{1}{n}(\zeta_i^n-\zeta_{i-1}^n) \quad (n=1, 2, \cdots, 5)$$

$$\zeta_{n,i}^*=\zeta_{n,i}-\frac{1}{a}(\omega_\xi-\omega_\theta)\zeta_{n+1,i}+\frac{\omega_\xi}{a^2}(\omega_\xi-\omega_\theta)\zeta_{n+2,i}, \quad \zeta_{n,i}^{**}=\zeta_{n,i}-\frac{1}{a}(\omega_\theta-\omega_\xi)\zeta_{n+1,i}+\frac{\omega_\theta}{a^2}(\omega_\theta-\omega_\xi)\zeta_{n+2,i} \quad (n=1, 2, 3) \tag{22}$$

and

$$\dot{N}^{vp}=\{\dot{N}_\xi^{vp}, \dot{N}_\theta^{vp}, \dot{N}_{\xi\theta}^{vp}, \dot{N}_{\theta\xi}^{vp}, \dot{Q}_\xi^{vp}, \dot{Q}_\theta^{vp}\}^T=\int_{-h/2}^{h/2}[L_1]\{\dot{\sigma}^{vp}\}d\zeta=\sum_{i=1}^{n}\int_{\zeta_{i-1}}^{\zeta_i}[L_1][D_i]\{\dot{\varepsilon}_i^{vp}\}d\zeta$$

$$\dot{M}^{vp}=[\dot{M}_\xi^{vp}, \dot{M}_\theta^{vp}, \dot{M}_{\xi\theta}^{vp}, \dot{M}_{\theta\xi}^{vp}\}^T=\int_{-h/2}^{h/2}[L_2]\{\dot{\sigma}^{vp}\}^*\zeta d\zeta=\sum_{i=1}^{n}\int_{\zeta_{i-1}}^{\zeta_i}[L_2][\bar{D}_i]\{\dot{\varepsilon}_i^{vp}\}^*\zeta d\zeta \tag{23}$$

$$[\bar{D}_i]=\frac{E_i}{1-\nu_i^2}\begin{bmatrix}1 & \nu_i & 0\\ \nu_i & 1 & 0\\ 0 & 0 & 1-\nu_i\end{bmatrix}$$

In Eqs.(19)～(23), the subscript i refers to the i th layer.

If $i=1$, $\zeta_1=h/2$ and $\zeta_0=-h/2$ are assumed in Eqs.(19)～(23), they coincide with the equations for the ordinary single-layered shells previously derived[9].

A complete set of field equations for 50 independent variables, $\dot{U}_\xi$, $\dot{U}_\theta$, $\dot{U}_\zeta$, $\dot{\Phi}_\xi$, $\dot{\Phi}_\theta$ $\dot{\Phi}_n$, $\{\dot{N}\}$, $\{\dot{N}^{vp}\}$, $\{\dot{M}\}$, $\{\dot{M}^{vp}\}$, $\{\dot{\varepsilon}_m\}$, $\{\dot{x}\}$, $\{\dot{\varepsilon}^{vp}\}$, $\{\dot{\sigma}\}$, $\{\dot{\sigma}^{vp}\}$, is now given by 50 equations, Eqs. (2), (5)～(8), (12), (15), (17) and (23).

2.2 Non-dimensional equations

It is assumed that the distributed loads and the 45 independent variables, except $\{\dot{\varepsilon}^{vp}\}$, can be expanded into Fourier series as follows:

$$\{\dot{P}_\xi, \dot{P}_\zeta\}=\frac{\sigma_0 h_0}{a}\sum_{n=0}^{\infty}\{\dot{p}_\xi^{(n)}, \dot{p}_\zeta^{(n)}\}\cos n\theta, \quad \dot{P}_\theta=\frac{\sigma_0 h_0}{a}\sum_{n=1}^{\infty}\dot{p}_\theta^{(n)}\sin n\theta$$

$$\{\dot{N}_\xi, \dot{N}_\xi^{vp}, \dot{N}_\theta, \dot{N}_\theta^{vp}, \dot{Q}_\xi, \dot{Q}_\xi^{vp}\}=\sigma_0 h_0\sum_{n=0}^{\infty}\{\dot{n}_\xi^{(n)}, \dot{n}_\xi^{vp(n)}, \dot{n}_\theta^{(n)}, \dot{n}_\theta^{vp(n)}, \dot{q}_\xi^{(n)}, \dot{q}_\xi^{vp(n)}\}\cos n\theta$$

$$\{\dot{N}_{\xi\theta}, \dot{N}_{\xi\theta}^{vp}, \dot{N}_{\theta\xi}, \dot{N}_{\theta\xi}^{vp}, \dot{Q}_\theta, \dot{Q}_\theta^{vp}\}=\sigma_0 h_0\sum_{n=1}^{\infty}\{\dot{n}_{\xi\theta}^{(n)}, \dot{n}_{\xi\theta}^{vp(n)}, \dot{n}_{\theta\xi}^{(n)}, \dot{n}_{\theta\xi}^{vp(n)}, \dot{q}_\theta^{(n)}, \dot{q}_\theta^{vp(n)}\}\sin n\theta$$

$$\{\dot{M}_\xi, \dot{M}_\xi^{vp}, \dot{M}_\theta, \dot{M}_\theta^{vp}\}=\frac{\sigma_0 h_0^3}{a}\sum_{n=0}^{\infty}\{\dot{m}_\xi^{(n)}, \dot{m}_\xi^{vp(n)}, \dot{m}_\theta^{(n)}, \dot{m}_\theta^{vp(n)}\}\cos n\theta$$

$$\{\dot{M}_{\xi\theta}, \dot{M}_{\xi\theta}^{vp}, \dot{M}_{\theta\xi}, \dot{M}_{\theta\xi}^{vp}\}=\frac{\sigma_0 h_0^3}{a}\sum_{n=1}^{\infty}\{\dot{m}_{\xi\theta}^{(n)}, \dot{m}_{\xi\theta}^{vp(n)}, \dot{m}_{\theta\xi}^{(n)}, \dot{m}_{\theta\xi}^{vp(n)}\}\sin n\theta$$

$$\left.\begin{aligned}
&\{\dot{U}_\xi,\ \dot{U}_\zeta,\ \dot{\varepsilon}_{\xi m},\ \dot{\varepsilon}_{\theta m},\ \dot{\varepsilon}_{\xi\zeta m},\ \dot{\varkappa}_\xi,\ \dot{\varkappa}_\theta,\ \dot{\Phi}_\xi\}=\frac{\sigma_0}{E_0}\sum_{n=0}^{\infty}\{a\dot{u}_\xi^{(n)},\ a\dot{u}_\zeta^{(n)},\ \dot{e}_{\xi m}^{(n)},\ \dot{e}_{\theta m}^{(n)},\ \dot{e}_{\xi\zeta m}^{(n)},\ \frac{\dot{k}_\xi^{(n)}}{a},\ \frac{\dot{k}_\theta^{(n)}}{a},\ \dot{\varphi}_\xi^{(n)}\}\cos n\theta\\
&\{\dot{U}_\theta,\ \dot{\varepsilon}_{\xi\theta m},\ \dot{\varepsilon}_{\theta\zeta m},\ \dot{\varkappa}_{\xi\theta},\ \dot{\varkappa}_{\theta\xi},\ \dot{\Phi}_\theta,\ \dot{\Phi}_n\}=\frac{\sigma_0}{E_0}\sum_{n=1}^{\infty}\{a\dot{u}_\theta^{(n)},\ \dot{e}_{\xi\theta m}^{(n)},\ \dot{e}_{\theta\zeta m}^{(n)},\ \frac{\dot{k}_{\xi\theta}^{(n)}}{a},\ \frac{\dot{k}_{\theta\xi}^{(n)}}{a},\ \dot{\varphi}_\theta^{(n)},\ \dot{\varphi}_n^{(n)}\}\sin n\theta\\
&\{\dot{\sigma}_\xi,\ \dot{\sigma}_\xi^{vp},\ \dot{\sigma}_\theta,\ \dot{\sigma}_\theta^{vp},\ \dot{\sigma}_{\xi\zeta},\ \dot{\sigma}_{\xi\zeta}^{vp}\}=\sigma_0\sum_{n=0}^{\infty}\{\dot{s}_\xi^{(n)},\ \dot{s}_\xi^{vp(n)},\ \dot{s}_\theta^{(n)},\ \dot{s}_\theta^{vp(n)},\ \dot{s}_{\xi\zeta}^{(n)},\ \dot{s}_{\xi\zeta}^{vp(n)}\}\cos n\theta\\
&\{\dot{\sigma}_{\xi\theta},\ \dot{\sigma}_{\xi\theta}^{vp},\ \dot{\sigma}_{\theta\zeta},\ \dot{\sigma}_{\theta\zeta}^{vp}\}=\sigma_0\sum_{n=1}^{\infty}\{\dot{s}_{\xi\theta}^{(n)},\ \dot{s}_{\xi\theta}^{vp(n)},\ \dot{s}_{\theta\zeta}^{(n)},\ \dot{s}_{\theta\zeta}^{vp(n)}\}\sin n\theta
\end{aligned}\right\}\tag{24}$$

where σ_0, h_0 and E_0 are a reference stress, a reference thickness, and a reference Young's modulus, respectively.

It should be noted that the Fourier expansions (24) are not the most general that could exist. For full generality, these expansions should be augmented by the additional series, e.g.,

$$\{\dot{P}_\xi,\ \dot{P}_\zeta\}=(\sigma_0h_0/a)\sum_{n=1}^{\infty}\{\dot{\bar{p}}_\xi^{(n)},\ \dot{\bar{p}}_\zeta^{(n)}\}\sin n\theta,\quad \dot{P}_\theta=(\sigma_0h_0/a)\sum_{n=0}^{\infty}\dot{\bar{p}}_\theta^{(n)}\cos n\theta.\tag{25}$$

Substituting these Fourier series into the above fundamental equations, the equations among the Fourier coefficients relating to the variables are obtained. Eliminating appropriately the coefficients, the resultant set for the displacement rates $\dot{u}_\xi$, $\dot{u}_\theta$, $\dot{u}_\zeta$, and the rotation rates $\dot{\varphi}_\xi$, $\dot{\varphi}_\theta$ can then be derived as follows :

$$\left.\begin{aligned}
&a_1\dot{u}_\xi''+a_2\dot{u}_\xi'+a_3\dot{u}_\xi+a_4\dot{u}_\theta'+a_5\dot{u}_\theta+a_6\dot{u}_\zeta'+a_7\dot{u}_\zeta+a_8\dot{\varphi}_\xi''+a_9\dot{\varphi}_\xi'+a_{10}\dot{\varphi}_\xi+a_{11}\dot{\varphi}_\theta'+a_{12}\dot{\varphi}_\theta=c_1\\
&a_{13}\dot{u}_\xi'+a_{14}\dot{u}_\xi+a_{15}\dot{u}_\theta''+a_{16}\dot{u}_\theta'+a_{17}\dot{u}_\theta+a_{18}\dot{u}_\zeta'+a_{19}\dot{\varphi}_\xi'+a_{20}\dot{\varphi}_\xi+a_{21}\dot{\varphi}_\theta''+a_{22}\dot{\varphi}_\theta'+a_{23}\dot{\varphi}_\theta=c_2\\
&a_{24}\dot{u}_\xi'+a_{25}\dot{u}_\xi+a_{26}\dot{u}_\theta+a_{27}\dot{u}_\zeta''+a_{28}\dot{u}_\zeta'+a_{29}\dot{u}_\zeta+a_{30}\dot{\varphi}_\xi'+a_{31}\dot{\varphi}_\xi+a_{32}\dot{\varphi}_\theta=c_3\\
&a_{33}\dot{u}_\xi''+a_{34}\dot{u}_\xi'+a_{35}\dot{u}_\xi+a_{36}\dot{u}_\theta'+a_{37}\dot{u}_\theta+a_{38}\dot{u}_\zeta'+a_{39}\dot{u}_\zeta+a_{40}\dot{\varphi}_\xi''+a_{41}\dot{\varphi}_\xi'+a_{42}\dot{\varphi}_\xi+a_{43}\dot{\varphi}_\theta'+a_{44}\dot{\varphi}_\theta=c_4\\
&a_{45}\dot{u}_\xi'+a_{46}\dot{u}_\xi+a_{47}\dot{u}_\theta''+a_{48}\dot{u}_\theta'+a_{49}\dot{u}_\theta+a_{50}\dot{u}_\zeta+a_{51}\dot{\varphi}_\xi'+a_{52}\dot{\varphi}_\xi+a_{53}\dot{\varphi}_\theta''+a_{54}\dot{\varphi}_\theta'+a_{55}\dot{\varphi}_\theta=c_5
\end{aligned}\right\}\tag{26}$$

where the superscript (n) on Fourier coefficients will be omitted for convenience. $a_1\sim a_{55}$ are the coefficients determined from the shell geometries and the elastic constants, E_i, ν_i. $c_1\sim c_5$ are constants determined from the distributed loads and the internal forces due to visco-plasticity in addition to the shell geometries. These are given as follows :

$$\left.\begin{aligned}
&c_1=\dot{n}_\xi^{vp\prime}+\gamma(\dot{n}_\xi^{vp}-\dot{n}_\theta^{vp})+\frac{n}{\rho}\dot{n}_{\theta\xi}^{vp}+\omega_\xi\dot{q}_\xi^{vp}-\dot{p}_\xi,\quad c_2=\dot{n}_{\xi\theta}^{vp\prime}+\gamma(\dot{n}_{\xi\theta}^{vp}+\dot{n}_{\theta\xi}^{vp})-\frac{n}{\rho}\dot{n}_\theta^{vp}+\omega_\theta\dot{q}_\theta^{vp}-\dot{p}_\theta\\
&c_3=\dot{q}_\xi^{vp\prime}+\gamma\dot{q}_\xi^{vp}+\frac{n}{\rho}\dot{q}_\theta^{vp}-\omega_\xi\dot{n}_\xi^{vp}-\omega_\theta\dot{n}_\theta^{vp}-\dot{p}_\zeta,\quad c_4=\dot{q}_\xi^{vp}-\lambda^2\dot{m}_\xi^{vp\prime}-\lambda^2\gamma\dot{m}_\xi^{vp}+\lambda^2\gamma\dot{m}_\theta^{vp}-\lambda^2\frac{n}{\rho}\dot{m}_{\theta\xi}^{vp}\\
&c_5=\dot{q}_\theta^{vp}-\lambda^2\dot{m}_{\xi\theta}^{vp\prime}-\lambda^2\gamma(\dot{m}_{\xi\theta}^{vp}+\dot{m}_{\theta\xi}^{vp})+\lambda^2\frac{n}{\rho}\dot{m}_\theta^{vp}
\end{aligned}\right\}\tag{27}$$

where $\lambda=h/a$.

The rates of internal forces related to visco-plasticity in Eqs.(27) become the following by the use of Eqs. (23) and (24):

$$\left.\begin{aligned}
&\sigma_0h_0\sum_{n=0}^{\infty}[A_n]\{\dot{n}_\xi^{vp(n)},\ \dot{n}_\theta^{vp(n)},\ \dot{n}_{\xi\theta}^{vp(n)},\ \dot{n}_{\theta\xi}^{vp(n)},\ \dot{q}_\xi^{vp(n)},\ \dot{q}_\theta^{vp(n)}\}^T=\sum_{i=1}^{n}\int_{\zeta_{i-1}}^{\zeta_i}[L_1][D_i]\{\dot{\varepsilon}^{vp}\}d\zeta\\
&\frac{\sigma_0h_0^3}{a}\sum_{n=0}^{\infty}[B_n]\{\dot{m}_\xi^{vp(n)},\ \dot{m}_\theta^{vp(n)},\ \dot{m}_{\xi\theta}^{vp(n)},\ \dot{m}_{\theta\xi}^{vp(n)}\}^T=\sum_{i=1}^{n}\int_{\zeta_{i-1}}^{\zeta_i}[L_2][\bar{D}_i]\{\dot{\varepsilon}^{vp}\}^*\zeta d\zeta\\
&[A_n]=[\cos n\theta,\cos n\theta,\sin n\theta,\sin n\theta,\cos n\theta,\sin n\theta]\\
&[B_n]=[\cos n\theta,\cos n\theta,\sin n\theta,\sin n\theta]
\end{aligned}\right\}\tag{28}$$

where $[A_n]$ and $[B_n]$ are diagonal matrices. The visco-plastic strain rates on the right-hand sides of Eqs.(28) can be related to the stresses by Eqs.(13). The integrations are carried out numerically by the use of Simpson's 1/3 rule.

3. Numerical Method

A finite difference method is employed for the solution of Eqs.(26). The usual central difference formulas are used for every mesh point except the discontinuity points and the boundary points of the shell. For the discontinuity points and the boundary points, forward and backward difference equations are employed[5]. Applying these difference formulas to fundamental equations (26), the boundary conditions and the continuity equations, the simultaneous equations can be obtained. The solutions at any stage of the problem are obtained by a summation of the increments of internal forces and displacements due to the load increment and the time increment.

4. Numerical Example

As a numerical example of the multi-layered shells of revolution, a simply supported two-layered cylindrical shell composed of mild steel and titanium subjected to locally distributed loads is considered

(Fig. 3). Three cases of the ratio of the thickness of the titanium layer to the shell thickness, $h_1/h=0$, 0.1, 0.3, are calculated.

It is sufficient to calculate only one-eighth of the shell with consideration of the symmetry of the problem. The geometrical parameters of this shell are as follows :

$$\left.\begin{aligned} &a=L,\ \xi=s/L,\ \rho=1/3,\ \omega_\theta=3 \\ &\rho'=\gamma=\omega_\xi=\omega'_\xi=0 \end{aligned}\right\} \tag{29}$$

The meridional mesh interval Δ in the finite difference calculation is

$$\Delta=1/2(N-1) \tag{30}$$

where N is the number of mesh points.

The boundary conditions at the points A ($i=1$) and B($i=N$) are, respectively,

$$\dot{U}_\xi=\dot{U}'_\zeta=\dot{\Phi}_\xi=\dot{N}_{\xi\theta}=\dot{M}_{\xi\theta}=0, \tag{31}$$

and

$$\dot{U}_\theta=\dot{U}_\zeta=\dot{M}_\xi=\dot{\Phi}_\theta=\dot{N}_\xi=0. \tag{32}$$

When $t=0$, the dots in the above equations are removed. The value of σ_0 in Eqs.(24) has been selected as $\sigma_0=1$ in this calculation.

The material constants of mild steel and titanium employed in the calculations are as follows[15],[16] :

Titanium :

$$\left.\begin{aligned} &E=9.1\times10^4\ \text{MPa} \\ &\nu=0.33,\ \gamma_1=800/\text{s} \\ &\Phi(F)=\{(\bar{\sigma}-\sigma^*)/\sigma^*\}^{7.4} \\ &\sigma^*=656(0.0101+\bar{\varepsilon}^{vp})^{0.252}\ \text{MPa} \\ &\text{Initial yielding stress}\quad \sigma_Y=206.1\ \text{MPa} \end{aligned}\right\} \tag{33}$$

Mild steel :

$$\left.\begin{aligned} &E=2.0\times10^5\ \text{MPa} \\ &\nu=0.29,\ \gamma_1=40.4/\text{s} \\ &\Phi(F)=\{(\bar{\sigma}-\sigma^*)/\sigma^*\}^{5.0} \\ &\sigma^*=261.7\ \text{MPa} \end{aligned}\right\} \tag{34}$$

The stress-strain curves for these material constants are shown in Fig. 4.

The meridional mesh point number N and division number K through the thickness are chosen to be $N=101$ and $K=11$ for each layer ($K=19$ in the case of $h_1/h=0$). The number of terms of Fourier series [$=(n+2)/2$)] is selected as $n=38$.

The increment of time Δt_j is decided as $\Delta t_j=0.9\Delta t_0$, where

$$\Delta t_0=\frac{4(1+\nu)}{3\gamma_0 E}\left(\frac{\sigma^*}{d\Phi/dF}\right)_j \quad (j:\text{calculation stage}) \tag{35}$$

is the stability limit given by Zienkiewicz and Cormeau[17]. It is regarded that the stationary state has been reached when the ratio of maximum visco-plastic strain rate $\dot{\varepsilon}^{vp}_{\max}$ to maximum strain $\varepsilon_{\max}$ immediately after each loading becomes less than 1.0×10^{-4}, *i. e.*, $|\dot{\varepsilon}^{vp}_{\max}/\varepsilon_{\max}|\leqq1.0\times10^{-4}$.

These values are determined according to the convergency of the solution, the capacity of the computer and computing time.

Some of the essential features of the solutions are shown in Figs. 5~14. In the figures, the broken lines indicate the values immediately after loading of P_1 and P_2, and the solid lines and chain lines indicate the values in stationary states. The results from thin shell theory (classical theory), which neglects the effect of shear deformations, are plotted by chain lines. P_0 and P_{0c} denote the initial yielding loads calculated from the present theory, and thin shell theory, respectively. In either theory, initial yielding occurs on the outer surface at point A ($\xi=0$, $\theta=0°$).

Figures 5(a) and (b) show the deformations of the meridional section $\theta=0°$ and those of the cross section $\xi=0$ with time, respectively. The dotted lines indicate the particle path. The shell is greatly deformed near point A ($\xi=0$, $\theta=0°$). The difference between the instantaneous state and the stationary state increases due to the progression of yielding with increasing loads. Shell deformations become large

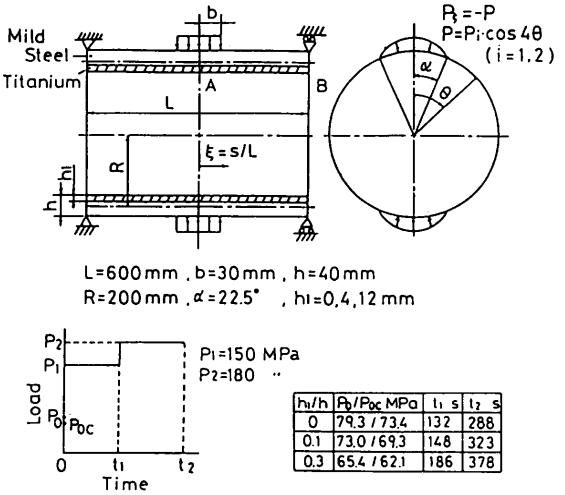

h_1/h	P_0/P_{0c} MPa	t_1 s	t_2 s
0	79.3 / 73.4	132	288
0.1	73.0 / 69.3	148	323
0.3	65.4 / 62.1	186	378

Fig. 3 Numerical example (two-layered cylindrical shell)

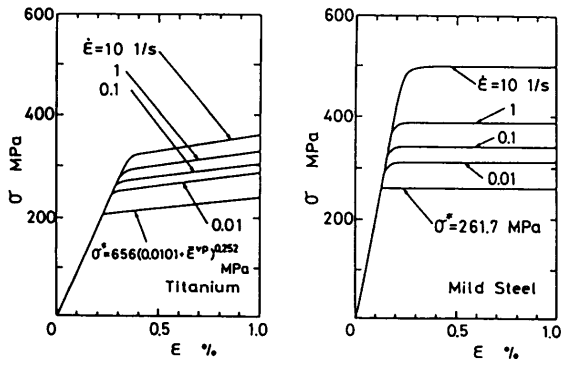

(a) Titanium (b) Mild steel

Fig. 4 Stress-strain relationships

with the increased thickness of the titanium layer. Some differences between the results from the present theory and the thin shell theory are seen in the loading parts of the shell.

Figures 6~9 represent the meridional and circumferential distributions of the resultant stresses. N_ξ and N_θ relax greatly in the loading parts, and the amount of relaxation increases a little with the thickness of the titanium layer A large difference between solutions from both theories is found in the loading part, and N_θ shows a more remarkable difference than N_ξ. Other resultant stresses have small values, small variation with time and little difference due to h_1/h.

Figures 10~12 are the variations of distributions of the resultant moments with time. M_ξ and M_θ relax largely with time in the loading parts, and M_θ relaxes more than M_ξ . The variations increase a little with h_1/h, but there is little difference between the stationary values at each loading stage. $M_{\xi\theta}$ and $M_{\theta\xi}$ are nearly equal, and these values and variations with time are both small. A relatively small difference between solutions from the two theories is observed in all the resultant moments.

Figures 13 (a) and (b) represent the distributions of stresses σ_ξ and σ_θ through the thickness at point A of the shell. The stresses relax in the outer part of the mild steel layer in every case of h_1/h. In the titanium layer, the stress variation is complex. The difference between solutions from two theories becomes significant near the boundary of elastic and plastic zones.

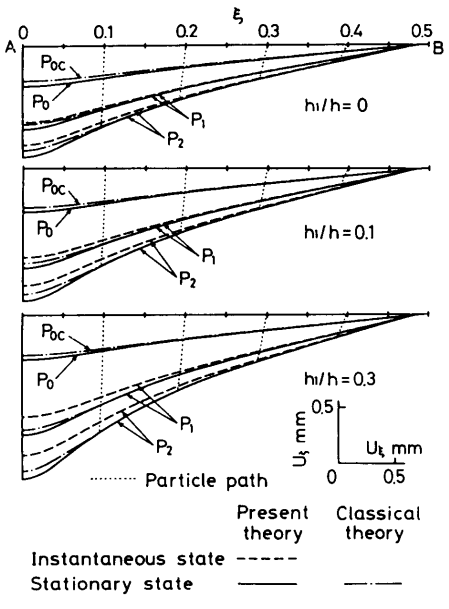

(a) $\theta=0°$

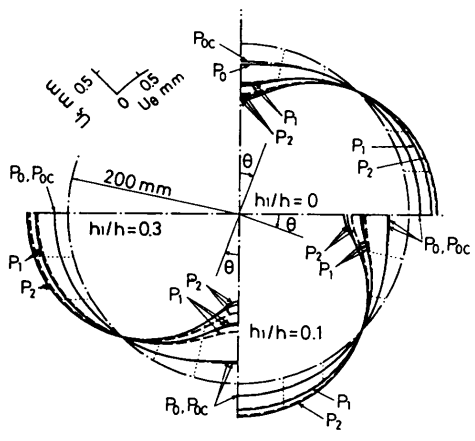

(b) $\xi=0$

Fig. 5 Deformations

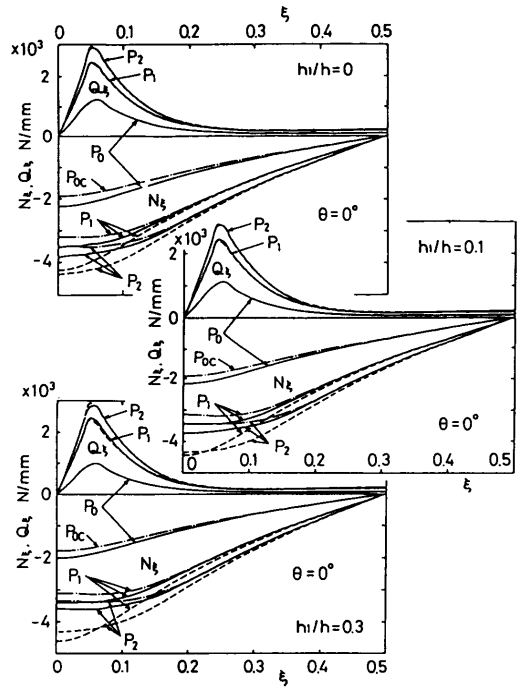

Fig. 6 Meridional distributions of N_ξ and Q_ξ

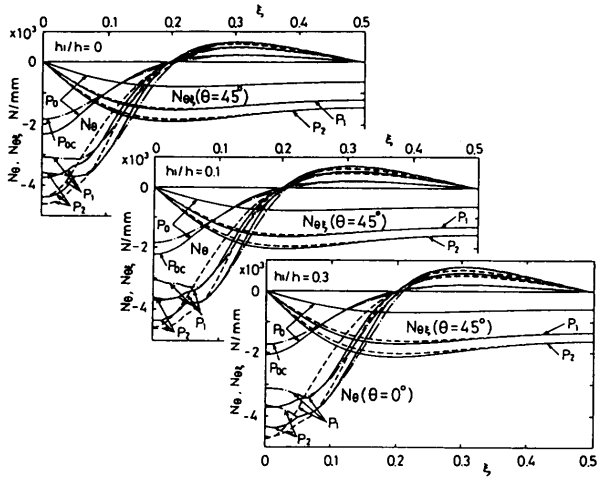

Fig. 7 Meridional distributions of N_θ and $N_{\theta\xi}$

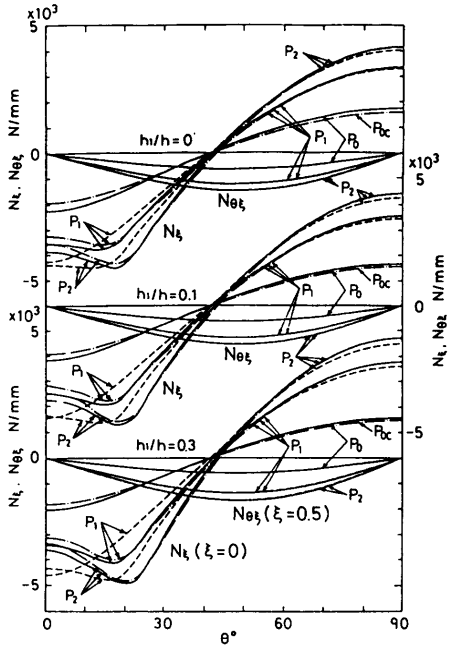

Fig. 8 Circumferential distributions of N_ℓ and $N_{\theta\ell}$

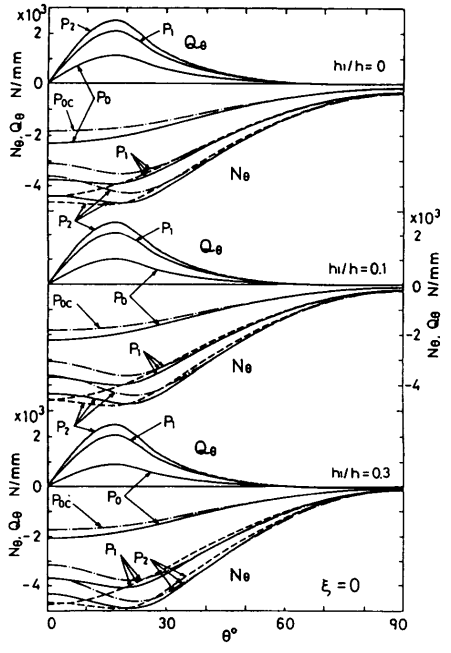

Fig. 9 Circumferential distributions of N_θ and Q_θ

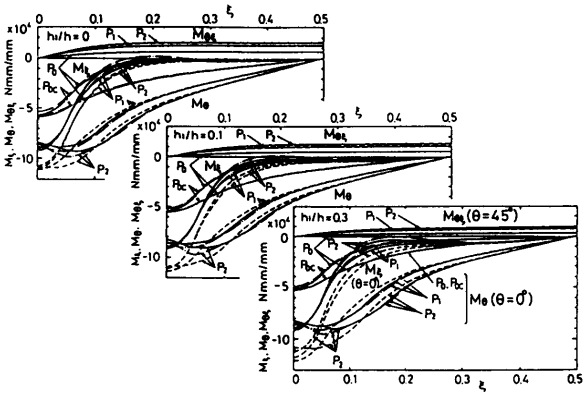

Fig. 10 Meridional distributions of M_ℓ, M_θ and $M_{\theta\ell}$

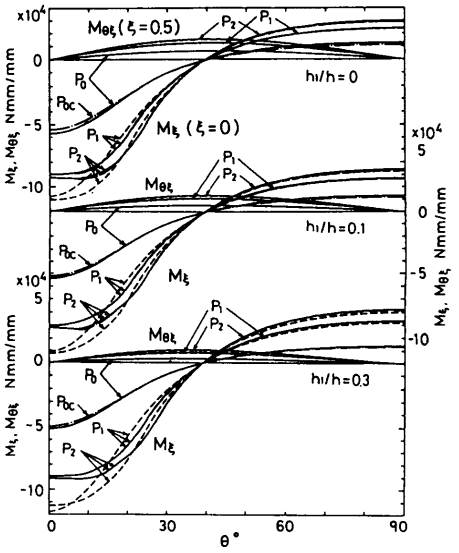

Fig. 11 Circumferential distributions of M_ℓ and $M_{\theta\ell}$

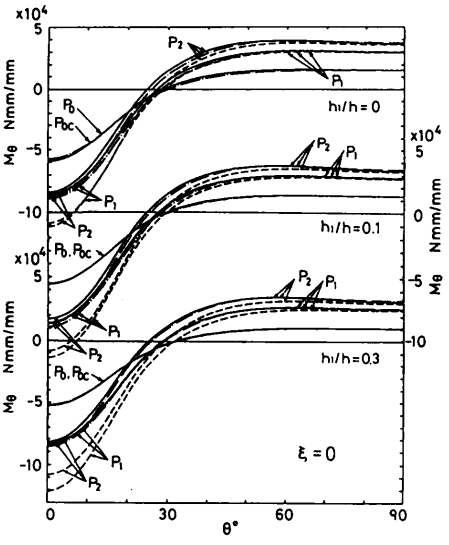

Fig. 12 Circumferential distributions of M_θ

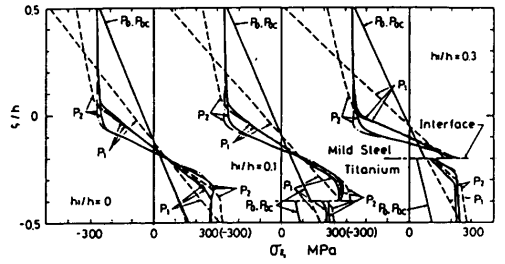

(a) σ_ξ

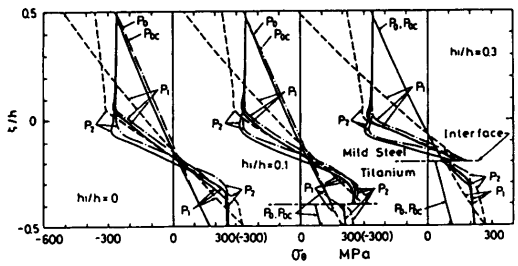

(b) σ_θ

Fig.13 Stress distributions through thickness at point A ($\xi=0$, $\theta=0°$)

Figure 14 illustrates the aspect of the progression of yielding. When $P=P_0$, the initial yielding occurs on the outer-surface at point A. With the increase of loads P, the plastic zones progress from the inner and outer surfaces of the loading part to the meridional, circumferential and thickness directions. The yielding zones of the two-layered shells are discontinuous on the interface and larger than those of the single-layered shell ($h_1/h=0$).

5. Conclusions

In this paper, the authors have described the numerical analysis of elasto/visco-plastic problems of multi-layered moderately thick shells of revolution under asymmetrical loads. The basic differential equations on the multi-layered shell have been developed on the basis of the Reissner-Naghdi theory for elastic moderately thick shells. The elasto/visco-plastic equations by Perzyna have been employed as the constitutive relation.

The increments of all pertinent variables have been expanded into Fourier series in the circumferential direction and decoupled sets of ordinary differential equations have been solved by the usual finite difference method. The solutions at any time are obtained by the integration of the incremental values.

As a numerical example of practical application, the elasto/visco-plastic deformation of a simply supported two-layered cylindrical shell composed of mild steel and titanium layers has been taken.

The numerical computations have been carried

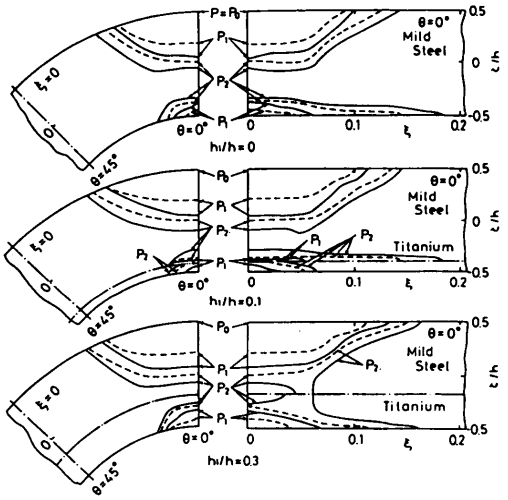

Fig. 14 Progressions of yield

out for three cases of the ratio of thickness of the titanium layer to shell thickness ($h/R=0.2$), and the results have been compared with those from the thin shell theory which neglects the effect of shear deformations. From the computations, the following was found :

(1) Deformation becomes large with the increase of h_1/h .

(2) The resultant stresses and the resultant moments are not influenced greatly by the ratio of the thickness of the titanium layer to the shell thickness. On the other hand, stress distributions through the thickness and progression of yield vary significantly depending on the thickness ratio.

(3) The difference between solutions from the present theory and those from the thin shell theory becomes significant.

References

(1) Zienkiewicz, O.C., Owen, D.R.J. and Cormeau, I.C., Analysis of Viscoplastic Effects in Pressure Vessels by the Finite Element Method, Nucl. Eng. & Desn., Vol.28(1974), p.278.

(2) Nagarajan, S. and Popov, E.P., Plastic and Viscoplastic Analysis of Axisymmetric Shells, Int. J. Solids and Struct., Vol.11(1975), p.1.

(3) Kanchi, M.B., Zienkiewicz, O.C. and Owen, D.R.J., The Visco-Plastic Approach to Problems of Plasticity and Creep Involving Geometric Non-Linear Effects, Int. J. for Numerical Methods in Eng., 12(1978), p.169.

(4) Takezono, S. and Akashi, T., Elasto/Visco-Plastic Deformations of Thin Shells of Revolution, Trans. 5th Int. Conf. Struct. Mech. in Reactor Technol., Vol.M(1979), M4/7.

(5) Tao, K. and Takezono, S., Elasto/Visco-Plastic Analysis of Axisymmetrical Shells under Asymmetrical Loading, Trans. 5th Int. Conf. Struct.

Mech. in Reactor Technol., Vol.M(1979), M4/8.
(6) Takezono, S. and Tanoue, M., Elasto/Visco-Plastic Analysis of Moderately Thick Shells of Revolution, Trans. 6th Int. Conf. Struct. Mech. in Reactor Technol., Vol.M(1981), M4/2.
(7) Atkatsh, R.S., Bieniek, M.P. and Sandler,I.S., Theory of Visco-Plastic Shells for Dynamic Response, ASME J. Appl. Mech., Vol.50, No.1 (1983), p.131.
(8) Kollmann, F.G. and Mukherjee, S., Inelastic Deformation of Thin Cylindrical Shells under Axisymmetric Loading, Ingenieur-Archiv, Vol.54 (1984), p.355.
(9) Tao, K., Takezono, S. and Nagano, S., Elasto/Visco-Plastic Analysis of Moderately Thick Shells of Revolution under Asymmetrical Loading, Trans. 9th Int. Conf. Struct. Mech. in Reactor Technol., Vol.B(1987), p.605.
(10) Takezono, S., Tao, K. and Nagano, S., Elasto/Visco-Plastic Analysis of Orthotropic Moderately Thick Shells of Revolution, Res Mechanica, Vol. 27(1989), p.335.
(11) Tao, K. and Takezono, S., Elasto/Visco-Plastic Analysis of Orthotropic Moderately Thick Shells of Revolution Under Asymmetrical Loading, Trans. 10 th Int. Conf. Struct. Mech. in Reactor Technol., Vol.B(1990), p.39.
(12) Takezono, S., Migita, K. and Hirakawa, A., Elasto/Visco-Plastic Deformation of Multi-Layered Shells of Revolution, JSME Int. J., Ser.I, Vol.31, No.3(1988), p.536.
(13) Reissner, E., A New Derivation of the Equations for the Deformation of Elastic Shells, Am. J. Math., Vol.63(1941), p.177.
(14) Naghdi, P.M., On the Theory of Thin Elastic Shells, Q. Appl. Math., Vol.14(1957), p.369.
(15) Perzyna, P., Fundamental Problems in Viscoplasticity, Adv. in Appl. Mech., Vol.9(1966), p.243, Academic Press.
(16) Takezono, S. and Satoh, M., Effect of Stress Frequency on Fatigue Crack Propagation in Titanium, ASME J. Eng. Mater. & Technol., Vol.104, No.4(1982), p.257.
(17) Zienkiewicz, O.C. and Cormeau, I.C., Visco-Plasticity-Plasticity and Creep in Elastic Solids-A Unified Numerical Solution Approach, Int. J. for Numerical Methods in Eng., Vol.8(1974), p.821.